International Journal of Thermophysics, Vol. 25, No. 6, November 2004 (© 2004)

Density and Thermal Expansion of Liquid Au–Cu Alloys

J. Brillo,[1,2] I. Egry,[1] H. S. Giffard,[1] and A. Patti[1]

Received December 29, 2003

The density of liquid Cu–Au alloys is measured using the technique of electromagnetic levitation, which entails producing a shadow image of the sample. The shadow is recorded by a digital CCD-camera, and the volume of the sample is calculated by an image processing algorithm. The density and thermal expansion of several alloys and the pure elements copper and gold are investigated at various temperatures above their melting points. In addition, the densities are also investigated as a function of the gold concentration at constant temperature. The measured values agree with literature data and with predictions obtained by molecular dynamics. It was found from data analysis that the ideal solution model applies.

KEY WORDS: Cu–Au alloys; density; electromagnetic levitation; ideal solution; thermal expansion; thermophysical properties.

1. INTRODUCTION

Thermophysical properties of liquid metals are important for both technical applications and physical understanding. In particular, the density has been measured by our group for a number of systems over the past couple of years [1–4]. These measurements were performed in an electromagnetic levitation chamber [1]. The aim of this work was to measure systems that have comparatively high densities, such as gold and Cu–Au alloys. Obviously, the force required to levitate a sample is proportional to its mass. Therefore, problems with the equilibrium position and visibility of gold–copper samples were to be expected. In addition, the low

[1]Deutsches Zentrum für Luft- und Raumfahrt, Institut für Raumsimulation, D-51170 Köln, Germany.
[2]To whom correspondence should be addressed. E-mail: Juergen.Brillo@dlr.de

0195-928X/04/1100-1881/0

emissivity and relatively low liquidus temperature of these alloys require an effective gas-cooling system. The Cu–Au system serves as a test system to explore the limits of our apparatus for samples of high densities. Furthermore, there are no experimental density data available for Cu–Au alloys. Therefore, another goal of this work is to fill that gap and produce reliable density data of Cu–Au alloys.

2. EXPERIMENTAL

All experiments presented in this work are carried out in an electromagnetic levitation chamber that is described in detail in Refs. 1–4. The density is measured using the arrangement shown in Fig. 1. The sample is levitated and melted under He/8vol%-H_2 with a current of 100 A and approximately 250 kHz applied to the coil. As soon as the electromagnetic forces levitate the sample, eddy currents, that are induced within, begin heating it. Temperature control is maintained by carefully cooling the sample in a laminar flow of the He/H_2 gas mixture, which is admitted from below via a ceramic tube. The temperature, T, is measured using an infrared pyrometer aimed at the top of the sample. For each sample, it is necessary to recalibrate the temperature with respect to the liquidus temperature, T_L, which is taken from Ref. 5. If T_P is the output signal from the pyrometer, then the real temperature T is obtained using the following approximation derived from Wien's law:

$$\frac{1}{T} - \frac{1}{T_P} = \frac{1}{T_L} - \frac{1}{T_{L,P}}. \tag{1}$$

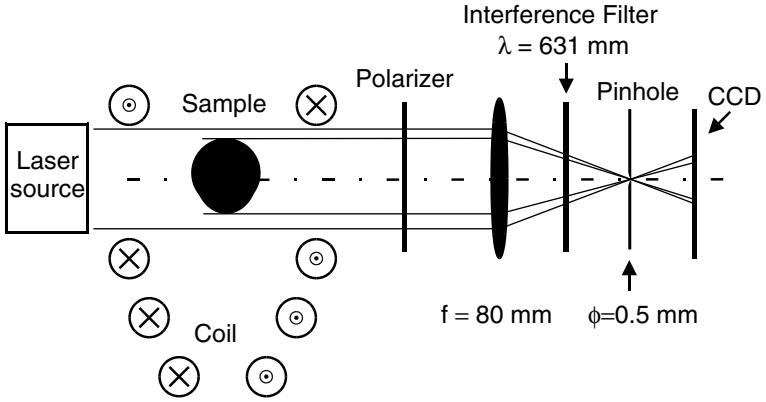

Fig. 1. Levitation technique for measuring density of molten alloys.

In Eq. (1), $T_{L,P}$ is the pyrometer signal at liquidus temperature, T_L. As shown in Fig. 2, $T_{L,P}$ is identified by a sudden change in the slope of T_P, that occurs upon melting when the sample temperature, T, exceeds T_L. Equation (1) is valid only if the sample emissivity at the operating wavelength of the pyrometer $\varepsilon_\lambda(T)$ remains constant over the experimentally scanned range of temperature. This is a good approximation for most metals; see Ref. 6. To measure the density based on the volume of the sample, it is of particular importance that the sample is fully visible from the side. A polarized HeNe laser beam, equipped with a spatial filter and a beam expander, is used to illuminate the sample from behind. Nonparallel components of the laser light are removed by a lens and a pinhole. The shadow image is captured by means of a digital CCD camera, and fed into a computer. It is analyzed by an edge detection algorithm that locates the edge curve $R(\varphi)$ by applying a spatial derivative operator to the image. $R(\varphi)$ is the edge curve in polar coordinates, R and φ, with respect to the drop center. In order to eliminate the influence of the droplet's oscillations, the edge curve is averaged over 1000 frames. The averaged edge curve is then fitted by Legendre polynomials of order $\leqslant 6$;

$$\langle R(\varphi)\rangle = \sum_{i=0}^{6} a_i P_i(\cos(\varphi)) \tag{2}$$

with P_i being the ith Legendre polynomial. As shown by a thorough analysis of top view images [1], the equilibrium shape of the sample is

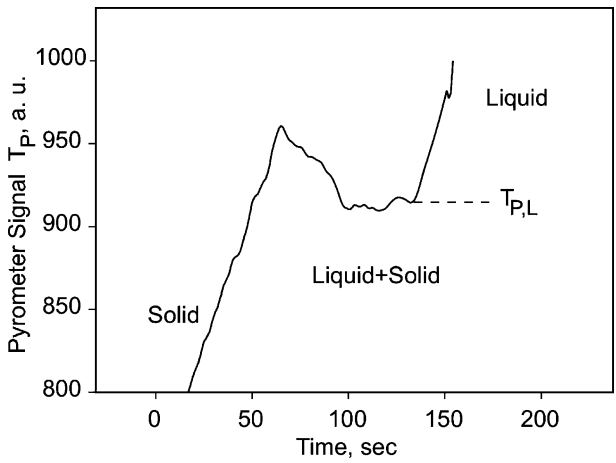

Fig. 2. Typical pyrometer output, T_P, when the sample melts. The value $T_{P,L}$ is used to calibrate the pyrometer signal with respect to the known liquidus temperature T_L.

symmetric with respect to the vertical axis. Hence, its volume is calculated using the following integral:

$$V_P = \frac{2}{3}\pi \int_0^{\pi} < R(\varphi) >^3 \sin(\varphi) d\varphi \tag{3}$$

V_P is the volume in pixel units.

In order to relate V_P to the real volume V, the system is calibrated using four different size ball bearings, placed in the laser beam. The bearings are manufactured with a tolerance [7] in diameter of 0.5–10 μm. Their volume is calculated from $V = qV_P$, with q being the scaling factor. When M is the mass of the sample, the density, ρ, is is calculated from $\rho = M/V$.

An absolute uncertainty analysis of the measurement technique is given in Ref. 2. It was found, that the relative deviation of the measured volumes $\Delta V/V$ is $\approx 0.1\%$, but the main source of error is the inaccuracy of the calibration factor $\Delta q/q$ which is approximately 1%. Hence, the total error for the density is $\Delta\rho/\rho \approx 1\%$.

Five different samples have been prepared with atomic gold-to-copper ratios of 0, 25, 50, 75, and 100 at% by alloying the required amounts of the constituent elements in an arc furnace. In order to check whether the mass of the sample remained constant over the duration of the experiment, each sample is weighed immediately before and after the measurement. In the case where the sample has lost more than $\approx 0.1\%$ of its initial mass, the measurement is disregarded.

3. RESULTS AND DISCUSSION

All samples could easily be levitated and were fully visible from the side. Figure 3 presents the measured densities of Cu–Au alloys vs. temperature. The analysis of the data indicates that the densities, ρ, can be described as linear functions of temperature, T, also shown in Fig. 3.

$$\rho(T) = \rho_L + \rho_T(T - T_L). \tag{4}$$

In this equation, ρ_L is the density at the liquidus temperature, T_L, and ρ_T is the thermal coefficient of the density. The parameters ρ_L, ρ_T, and T_L are listed in Table I for each sample. Obviously, the density increases with an increase of the gold content. Figure 4 shows the thermal coefficient, ρ_T, as a function of the atomic gold percentage, C_{Au}, and although there is a large scatter in the data, ρ_T generally decreases with increasing C_{Au}.

Our data are in good accordance with literature data. In particular, the values of pure copper and gold fit well to data measured by

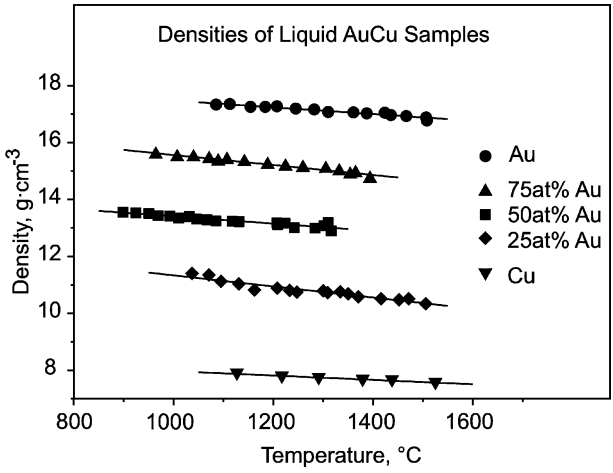

Fig. 3. Density data for levitated Cu–Au alloys at different temperatures.

means of sessile drop and maximum bubble pressure [8,9] methods; see Table II. To our knowledge, this is the first time that densities for Cu–Au alloys have been measured and, therefore, no experimental data are available for comparison. However, molecular dynamic simulations using the

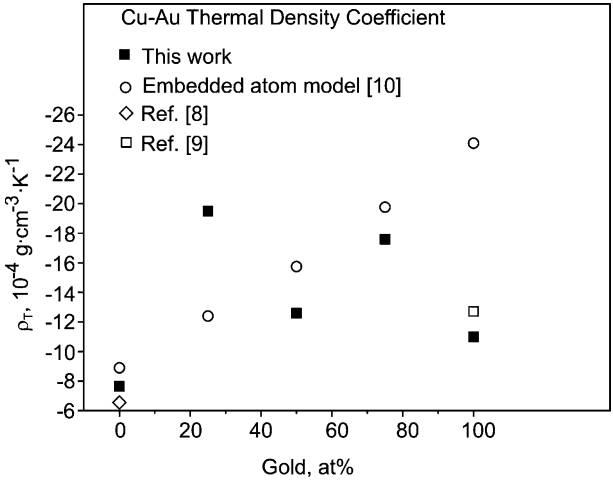

Fig. 4. Thermal coefficient, ρ_T, of Cu–Au as function of gold content in comparison with literature data [X. J. Han et al., Submitted].

Table I. Parameters ρ_L and ρ_T for each sample in comparison to results of Ref. [10]

Sample	T_L(°C)	This work		MD – simulation, [10]	
		ρ_L ($g \cdot cm^{-3}$)	ρ_T ($10^{-4}\, g \cdot cm^{-3} \cdot K^{-1}$)	ρ_L ($g \cdot cm^{-3}$)	ρ_T ($10^{-4}\, g \cdot cm^{-3} \cdot K^{-1}$)
Copper	1084	7.9	-7.7 ± 0.5	7.84	−8.91
CuAu-25at%	970	11.39	-19.5 ± 1.6	10.98	−12.39
CuAu-50at%	920	13.50	-12.6 ± 0.9	13.47	−15.75
CuAu-75at%	942	15.67	-17.6 ± 0.9	15.32	−19.77
Gold	1064	17.39	-11.0 ± 0.6	16.48	−24.12

Table II. Parameters ρ_L and ρ_T for the pure elements copper and gold in comparison to literature data

Sample	ρ_L ($g \cdot cm^{-3}$)	ρ_T($10^{-4}\, g \cdot cm^{-3} \cdot K^{-1}$)	Reference
Copper	7.901	-7.7 ± 0.5	This work
	7.835	−8.9	Molecular Dynamics [10]
	7.86	−6.6	[8]
Gold	17.39	-11.0 ± 0.6	This work
	16.48	−24.1	Molecular Dynamics [10]
	17.19	−12.7	[9]

embedded atom method were carried out just recently on this system [10]. The embedded atom method is a quasi-atom model beased on density functional theory. The energy of an atomic configuration is subdivided into a short range part due to a pairwise interaction of the cores and a so called embedding energy. The embedding energy is required to add one atom to the system with given local electron density, due to all other atoms. For a given alloy system, the functional dependence of the embedding energy is independent of the atomic concentrations of the elements, which makes the method attractive for the investigation of alloys. The results of these simulations fit well to our data (see Table I).

From the fit parameters, ρ_L and ρ_T, the density was calculated at $T = 1200°C$ for each concentration, and the results are shown in Fig. 5 together with the simulated [10] values. Again, from this figure, the good agreement with the predicted values is obvious, although the experimental

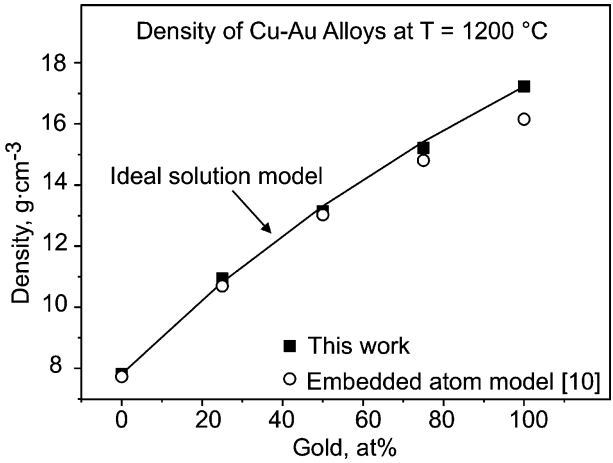

Fig. 5. Density, ρ, of Cu–Au at constant temperature $T = 1200°C$. Data are plotted as a function of gold content in comparison with literature data [10]. Solid line represents the interpolation given by Eq. (5).

results are slightly higher than the predicted values. In addition, our experimental values of ρ_T (shown in Fig. 4) are also in good agreement with the theoretically predicted ones, except for gold. For gold, our result for ρ_T agrees well with the experimental value of Ref. 9, whereas the MD simulation yields a value twice as large. This cannot be explained by experimental error and is probably due to the chosen parameters for gold in the MD simulation.

The molar volume of an alloy can generally be represented by [1]

$$V_{Cu/Au} = C_{Cu} V_{Cu} + C_{Au} V_{Au} + \Delta V, \tag{5}$$

where V_{Cu} and V_{Au} the molar volumes of the pure substances copper and gold at constant temperature T. C_{Cu} and C_{Au} are their atomic concentrations and ΔV is the excess volume. For $\Delta V = 0$, Eq. (5) reduces to a linear combination of the molar volumes, which in the following is referred to as the ideal solution model. (It should be noted here, that $\Delta V = 0$ is not equivalent to a zero energy of mixing, $\Delta G = 0$ [2].)

Since $\rho = M/V$, the ideal solution model is not identical to the Neumann–Kopp rule which assumes a linear combination of the densities. As shown in Fig. 5, Eq. (5) describes well the measured data with $\Delta V = 0$.

Whether or not an ideal behavior can be expected for atoms of different sizes by geometric arguments alone is controversial. Lemaignan [11]

investigated the packing density of binary mixtures of differently sized steel balls. He considered diameter ratios α, ranging from 0.5 to 0.945 and did not observe any significant change in the packing density for diameter ratios $\alpha > 0.7$, i. e., $\Delta V = 0$. As for the majority of metallic alloys the α is larger than 0.7, his conclusion was that a contribution to the excess volume due to geometric factors does practically not occur.

On the other hand, Khantadze and Topuridze [12] studied the same system. They however found, that there is a negative excess volume, $\Delta V < 0$, even for values of α very close to 1. For the gold–copper system, α is approximately 0.88 [13], and the two papers yield conflicting results.

4. SUMMARY

The five different samples, copper, gold, Cu-75at%Au-25at%, Cu-50at%Au-50at%, and Cu-25at%Au-75at%, can easily be levitated by our setup. For each sample, the density is described as a linear function of temperature. The measured densities increase with increasing gold content. Our results agree well with literature data and with predictions based on molecular dynamics simulations. It was found that the density of the Cu–Au system is described in terms of an ideal solution model and no excess volume is required.

REFERENCES

1. J. Brillo and I. Egry, *Int. J. Thermophys.***24**:1155 (2003).
2. J. Brillo and I. Egry, *Z. Metallkd.***95** (2004).
3. R. A. Harding, R. F. Brooks, G. Pottlacher, and J. Brillo, *Gamma Titanium Aluminides 2003*-TMS 2003-75 (2003).
4. J. Brillo, S. Schneider, I. Egry, and R. Harding, *in Proc. 10th Titanium World Conf.*, H. Lutjering, ed. (Wiley-VCH, Weinheim, in press).
5. T. B. Massalski, *Binary Alloy Phase Diagrams* (American Society for Metals, Materials Park, Ohio, 1986).
6. S. Krishnan, G. P. Hansen, R. H. Hauge, and J. L. Margrave, *High Temp. Sci.* **29**:17 (1990).
7. *International Organization for Standardization, Rolling Bearings – Radial Bearings – Tolerances*, ISO 492 (2002).
8. S. Watanabe and T. Saito, *J. Japan Inst. Metals* **35**:554 (1971).
9. G. P. Khilya, Yu. N. Ivashchenko, and V. N. Eremenko, *Izv. Akad. Nauk SSSR, Met.* **6**:87 (1975).
10. [X. J. Han et al., Submitted]
11. C. Lemaignan, *Acta Met.* **28**:1657 (1980).
12. D. V. Khantadze and N. I. Topuridze, *Zhurn. Fiz. Khim.* **33**:120 (1977)
13. R. P. Elliot, *Constitution of Binary Alloys* (McGraw Hill, New York, 1965)